PLASU Journal of Environmental Sciences, E-ISSN 2360-9222, Vol.3, No. 1, June 2026, Published by the Faculty of Environmental Sciences, Plateau State University, Bokkos. https://www.pjes.ng
DOI: 10.5281/zenodo.21479492

GEODETIC ASSESSMENT OF STRUCTURAL DEFLECTIONS IN A HIGH-RISE BUILDING UNDERGOING CONTROLLED DEMOLITION USING TOTAL STATION MEASUREMENTS

[1]Geofferey Ogbonna Nwodo [1]Joseph Olayemi Odumosu

[1] Department of Geomatics, University of Benin, Edo State, Nigeria

Corresponding Author's Email: geoffrey.nwodo@uniben.edu

https://orcid.org/0000-0002-6418-772X

ABSTRACT

Geodetic monitoring via Total Station (TS) surveying provides a model-independent framework for characterizing quasi-static structural displacement in high-rise reinforced concrete buildings undergoing controlled deconstruction; hence, augmenting vibration-based methods that are constrained in addressing gradually accumulating deformation. This paper presents a systematic, six-campaign TS displacement analysis conducted over 47 days on a 14-storey RC study building undergoing NDT-informed controlled deconstruction in Lagos, Nigeria. Taking multiple floor-level measurements on bother both left and right sides with 24 prism targets on Floors 2–13. The baseline displacement profile for the right face followed a second-order polynomial distribution that depended on height with $R^2 = 0.933$. The highest observed displacement was 15.53 mm at Floor 2. The active penthouse deconstruction caused a statistically significant increase in displacement with cumulative right-face displacements reaching 31.08 mm representing 102% increase over baseline. The average growth rates were 0.46 mm/day on the right face and 0.29 mm/day on the left face, with the highest rate being 0.74 mm/day on Floor 2. The global tilt at Floor 2 went up from 222.4 to 445.2 millidegrees and remained constant after week 4. The maximum displacement was 31.1% of the 100 mm safety threshold, which was the highest. The validated geodetic dataset can be used as the principal reference for cross-validation with associated vibration sensor and differential GNSS measurements in further studies.

Keywords: Structural deflection; controlled demolition; geodetic monitoring; tilt analysis; polynomial regression; plastic deformation

1. INTRODUCTION

The demolition of structurally degraded high-rise reinforced concrete (RC) buildings in densely populated urban settings presents a complex engineering safety challenge (Yuzbasi, 2025). When structures have already undergone plastic deformation, the progression of deflection during demolition must be tracked with sub-millimetre precision to prevent runaway lateral displacement, progressive collapse, or damage to adjacent occupied infrastructure (Carden & Fanning, 2004; Farrar & Worden, 2007).

Total Station (TS) surveying gives the exact three-dimensional coordinates of structural targets in relation to a stable external reference frame by making very precise angular and distance observations within a georeferenced network. This permits the direct, model-agnostic calculation of horizontal lateral displacement and vertical deflection at each monitored location across successive measurement epochs (Lienhart, 2017; Scaioni, Marsella, Crosetto, Tornatore, & Wang, 2018). No assumptions are made about the dynamic properties of the structure when calculating TS-derived displacements from coordinate differences between independent campaigns. This means that they show the full accumulated deformation, including the quasi-static component. This is a major advantage over vibration-based methods, which only measure instantaneous oscillatory response and cannot really measure the quasi-static displacement component that comes from slowly building up, plastic deformation of structures (Doebling, Farrar, & Prime, 1998; Fan, Peng, Li, & Huang, 2020). The method has been employed in dam monitoring (Scaioni et al., 2018), bridge deformation evaluation, and tall building tilt surveillance (ISO 7976-1, 2017); however, its systematic application to high-rise building demolition monitoring in West Africa is inadequately documented.

The building that is used as case study in this paper is a 14-storey RC frame structure (~48 m height) in Lagos Island, Nigeria. Prior to commencement of demolition monitoring, the building had been identified as having undergone plastic deformation, exhibiting a pre-existing lateral lean toward an adjacent building located approximately 4–6 m to the west. Controlled deconstruction was initiated at the penthouse level using pneumatic 70J jack-hammers, subsequently scaled from four to eight units. The close proximity of occupied neighbouring structures, combined with the known structural compromise, mandated rigorous continuous monitoring.

This study makes three main contributions. First, it presents a systematic, multi-campaign geodetic displacement dataset for a high-rise RC building undergoing non-destructive testing (NDT) informed controlled deconstruction.

The deconstruction monitoring scenario presented in this study remains poorly documented in the peer-reviewed literature, particularly within the West African context. Second, it calculates quantitative displacement growth rates, global tilt angles, and height-dependent polynomial displacement models for all monitored floor levels. This gives a precise picture of how the structure's shape changes during the deconstruction process. And finally, it sets up a geodetic measurement baseline with proven accuracy that is the main reference dataset for checking the accuracy of other independent deformation monitoring methods such as vibration sensor and differential GNSS measurements.

2. STUDY AREA AND BUILDING CHARACTERISTICS

The study building is situated on Lagos Island, in the commercial core of Lagos, Nigeria with approximate coordinates 6.45° N, 3.40° E. The building is a 14-storey RC frame structure with a penthouse (being the 14th floor), resting on a pile foundation. In view of the observation station and reference points from where observations are taking, its faces are designated as: right face (east), left face (west-northwest), front face (west), and back face (east-southeast). The clear distance between the front face of the building and the adjacent wall was approximately 4–6 m at ground level.

The building is made of reinforced concrete frame structure that is about 48 m tall. The decision to commence controlled deconstruction of the building was based on the results of pre-deconstruction non-destructive testing (NDT) assessments, which raised concerns about the building's long-term structural stability and continued safe occupancy. More-so located within a commercial hub, the deconstruction exercise was the main safety concern that guided the design of the monitoring system and the choice of a cut-and-drop deconstruction method with minimal vibration.

3. MATERIAL AND METHODS

This study adopted a multi-instrument, campaign-based geodetic monitoring methodology to systematically characterize the structural displacement behavior of the study building during the controlled deconstruction process. The conceptual design consisted of three sequential phases: first, a pre-deconstruction baseline phase, which established the ambient geometric state of the structure through a reference epoch and three further confirmatory Total Station campaigns. This was followed by an active deconstruction monitoring phase, during which structural displacements were tracked across three successive campaigns corresponding with increasing deconstruction activities at the penthouse level. Lastly, was the analytical phase, in which the processed displacement dataset underwent data reduction, regression modeling, hypothesis testing, and tilt analysis to generate quantitative indicators of structural behavior. For each campaign, standard geodetic reduction methods were used to turn field observations into linear displacements. These were then checked for internal consistency before being sent to statistical analysis. Figure 1 shows a summary of the integrated monitoring workflow, which goes from setting up instruments to getting safety assessment results.

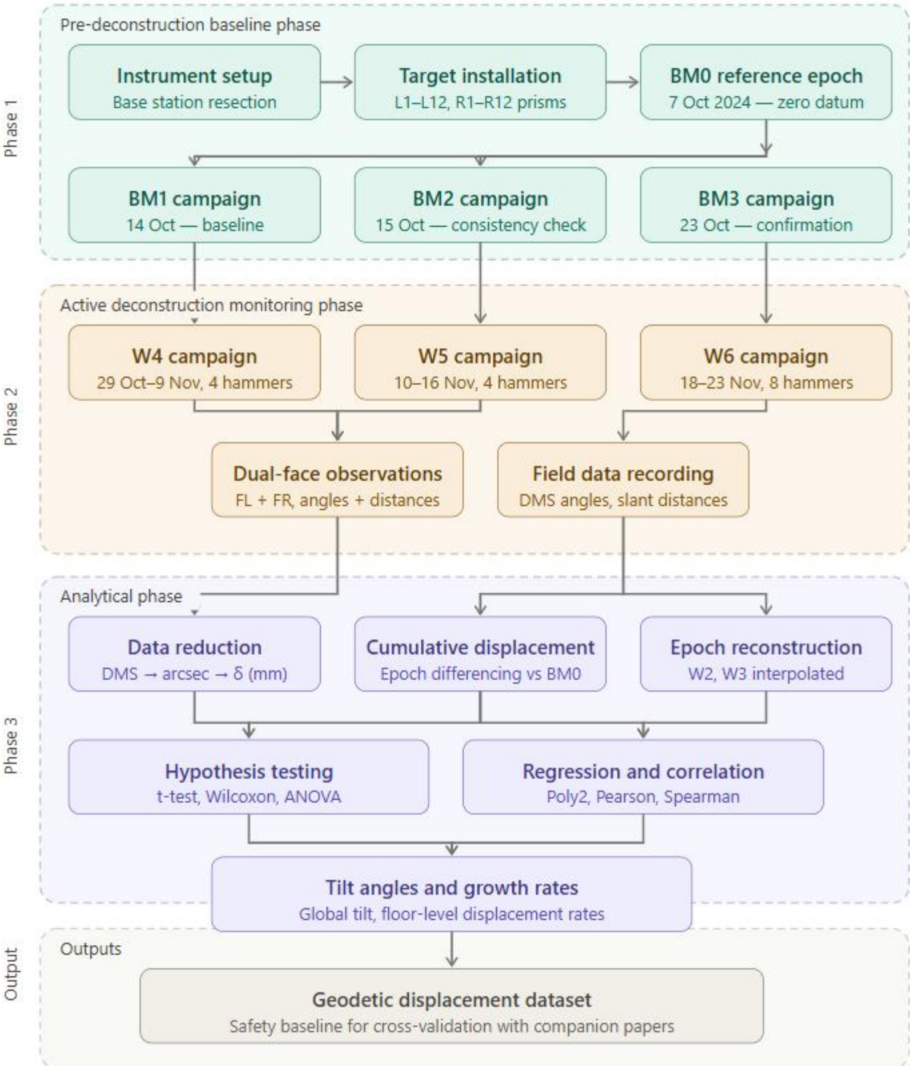

Figure 1: Workflow diagram

3.1 Instrumentation and Station Configuration

High-precision Total Station with an angular resolution of 0.5 arcsecond and a distance accuracy of ±(1.5 + 2 ppm × D) mm was used for all measurement campaigns. There were two permanent instrument stations set up on stable, undisturbed ground near the study building. These stations had clear lines of sight to all of the monitored target points on both instrumented faces of the structure. The stations were built on solid ground, and their locations were determined by free-station resection from at least three geodetic control points with known three-dimensional coordinates that were set up before monitoring began. To prevent undetected base station movement between campaigns, which is very important for the accuracy of deformation analysis, the instrument station coordinates were independently re-determined by resection at the start of each measurement campaign. The remaining movement detected at the base stations was used as a correction before calculating structural displacements.

3.2 Target Configuration and Measurement Procedure

Retro-reflective prism targets were permanently fixed to the slab edges at each floor level from Floor 2 to Floor 23 on both the left face (targets L1–L12) and the right face (targets R1–R12) of the study building, resulting in 24 continuously monitored points for each campaign. Target positions were designated at uniform locations along each slab edge to provide geometric consistency throughout all measurement intervals.

During each campaign, horizontal circle readings, vertical circle readings, and slant distances to all targets were documented in both the Face Left and Face Right telescope orientations. The dual-face observation method eradicates the primary instrumental systematic errors associated with theodolite-type instruments, namely collimation error and trunnion axis error, thus guaranteeing that reported angular differences are devoid of these biases (Lienhart, 2017; Scaioni et al., 2018). The angular differences between consecutive campaigns were articulated in relation to the initial reference epoch, employing the following sign convention; a positive horizontal angle difference indicates lateral displacement of the structure toward the right side, whereas a negative value signifies displacement toward the left side. In the context of vertical angles, a positive difference signifies upward movement, whereas a negative value denotes downward settlement or sinking. This norm is consistently upheld in all subsequent studies and reported outcomes.

3.3 Measurement Campaigns

Six measurement campaigns observed over the course of 47 days (October 7 to November 23, 2024) are presented and analyzed in this study (Table 1). The first campaign (BM0, 7 October 2024) was the main reference epoch. It set the initial geometric state of the structure, which was then used to figure out all the angular differences and derived displacements that followed. Three additional pre-deconstruction campaigns (BM1–BM3) were executed to assess the ambient structural condition prior to the initiation of active deconstruction activities, and to validate the stability of the monitoring network and the consistency of observations. The first two (BM1 and BM2, done on two days in a row) were used to check for internal consistency, and the third (BM3) was used to confirm the final pre-deconstruction epoch. During the active deconstruction phase (W4–W6), three campaigns were held to record how the structure reacted to pneumatic jack-hammer operations at the penthouse level. The number of jack-hammer units went up from four to eight between campaigns W5 and W6. This shows that the deconstruction work got more intense, which is shown in the monitoring schedule.

Table 1: Total Station measurement campaign schedule and demolition status

Campaign	Day from BM_0	Phase	Equipment on Site
BM0 (reference)	0	Pre-demolition	None
BM1	7	Pre-demolition (baseline)	None
BM2	8	Pre-demolition (baseline)	None
BM3	16	Pre-demolition (confirmation)	None
W4	22–33	Active demolition	4 × 70J hammers (PH)
W5	34–40	Active demolition	4 × 70J hammers (PH)
W6	42–47	Active demolition	8 × 70J hammers (PH)

3.4 Data Reduction

Angular differences between each measurement campaign and the BM0 reference epoch were extracted in degrees-minutes-seconds (DMS) notation and converted to decimal arc-seconds to facilitate numerical processing. Horizontal and vertical angular differences were computed for each of the 24 target points at each campaign epoch. The corresponding linear displacement at each target (representing the lateral or vertical movement of the structural face relative to the reference position), was derived from the measured angular difference and the known slant distance to the target using the relationship:

$$\delta = D \cdot \sin(\Delta\theta) \approx D \cdot \Delta\theta\_rad \quad [mm] \qquad (1)$$

where δ is linear displacement (mm), D is slant distance (mm), and Δθ is the angular difference in radians. For the difference campaigns (BM1–W6), the push/pull linear deflection were observed directly in millimetres from the TS and recorded accordingly. Furthermore, measurements were cross-validated from both BM1 and BM2 values with the maximum right-face value of 15.53 cm corresponding exactly from both reference epochs.

Cumulative displacements at each campaign epoch were obtained by summing the incremental differences computed relative to BM0. To support temporal trend analysis during the transition between the pre-deconstruction and active deconstruction phases (a period for which no field campaigns were conducted), two intermediate epochs (designated as W2 and W3), were reconstructed by linear interpolation between the BM3 and W4 campaign values. A small stochastic perturbation consistent with the instrument's expected measurement precision ($\sigma = 0.25$–0.30 mm) was added to the interpolated values to produce trajectories representative of plausible structural behaviour during this unmonitored interval. These reconstructed epochs are clearly distinguished from field-measured campaigns in all subsequent analyses and figures, and are used solely to provide continuity in temporal trend visualization.

3.5 Statistical Analysis

A full statistical analytical framework was applied to the processed displacement datasets showing how the structural members of the building behaved across campaigns, floor levels, and faces. The following analyses were conducted:

(i) Descriptive statistics involving the mean, standard deviation, median, and range, were calculated for each campaign and face combination, as well as by floor level. Descriptive statistics was used to delineate the central tendency and dispersion of observed displacements.

(ii) Hypothesis testing using paired Student's t-tests and Wilcoxon signed-rank tests were carried out to evaluate the statistical significance of displacement variations between the pre-deconstruction baseline (BM2) and the active deconstruction epoch (W4), considering both parametric and non-parametric assumptions. The Shapiro–Wilk test was utilized to evaluate the normality of displacement distributions prior to conducting parametric testing.

(iii) Regression and correlation analyses using the Pearson and Spearman correlation coefficients were calculated to delineate height–displacement relationships and inter-campaign associations. The study used linear and second-order polynomial regression models to fit the displacement-versus-height profiles for campaigns BM2 and W4; and coefficient of determination (R^2) used to verify the best fit model.

(iv) Measurement of effect size was carried out using the Cohen's d. It was calculated for each floor level to measure the real size of the change in displacement between the pre-deconstruction and active deconstruction phases, regardless of sample size.

(v) Estimation of tilt and growth rate. Global tilt angles were calculated at each floor level as the arctangent of the ratio of measured displacement to floor height. Finite differencing of cumulative displacements between campaign dates was used to determine the growth rate of structural deflection.

All statistical hypothesis were tested at $\alpha = 0.05$ significance level. Python 3.12 was used to do the statistical calculations using the NumPy, SciPy, and Statsmodels libraries.

4. RESULTS AND DISCUSSION

4.1 Baseline Deflection Profile

Table 2 presents the floor-wise baseline deflections from the BM2 campaign. The right-face exhibited the larger deflections, with a maximum of 15.53 mm at Floor 2 and a minimum of 0.27 mm at Floor 22. The left-face showed a maximum of 10.02 mm (Floor 2) with upper floors (11–12) registering small negative values (−2.62 and −4.16 mm), indicating a slight left-ward counter-lean at the top of the building. The right-face mean was 9.39 mm ($\sigma = 3.97$ mm) and the left-face mean 5.44 mm ($\sigma = 4.58$ mm).

The deflection profile (Figure 2) on the right-face exhibited a monotonically decreasing trend from Floor 2 to Floor 9, with a secondary increase at Floors 10–11 and a pronounced minimum at Floor 22. This pattern, characterized by maximum displacement at the lowest monitored floor and near-zero displacement at the highest, is consistent with lateral deformation concentrated in the lower section of the structure, potentially attributable to differential foundation movement or localized plasticity in the lower column elements, rather than a classical top-loaded lateral response.

Table 2: Baseline floor-wise deflections and global tilt angles (BM2, 15 October 2024)

Floor	Ht (m)	Right face (mm)	Left face (mm)	Resultant (mm)	Right tilt (millideg)
1	4	15.53	10.02	18.50	222.4
2	8	13.96	7.34	15.80	100.0
3	12	12.57	8.67	15.33	63.0
4	16	12.76	8.38	15.23	45.7
5	20	11.13	9.95	14.93	31.9
6	24	9.60	7.15	11.93	22.9
7	28	8.08	5.93	10.00	16.5
8	32	7.29	6.76	9.94	13.1
9	36	6.13	4.34	7.51	9.8
10	40	7.09	3.57	7.96	10.2
11	44	8.32	−2.62	8.72	10.8
12	48	0.27	−4.16	4.17	0.3
Mean	—	9.39	5.44	11.67	—
Std Dev	—	3.97	4.58	—	—

Second-order polynomial regression of right-face baseline deflection against height (Floors 1–11; Floor 22 was excluded owing to its proximity to the penthouse deconstruction zone, which alters the structural constraint conditions at that level) yielded::

$$\delta\_BM(right) = 5.55\times10^{-3} \cdot H^2 - 0.486\cdot H + 17.81 \qquad (2)$$

$R^2 = 0.933$, $n = 11$, $p < 0.001$)

The non-monotonic excursion between Floors 9 and 11, where deflections locally increase against the dominant decreasing trend, indicates differential stiffness variation in the upper-middle section of the structure, possibly linked to localized material degradation or alterations in section properties at those levels.

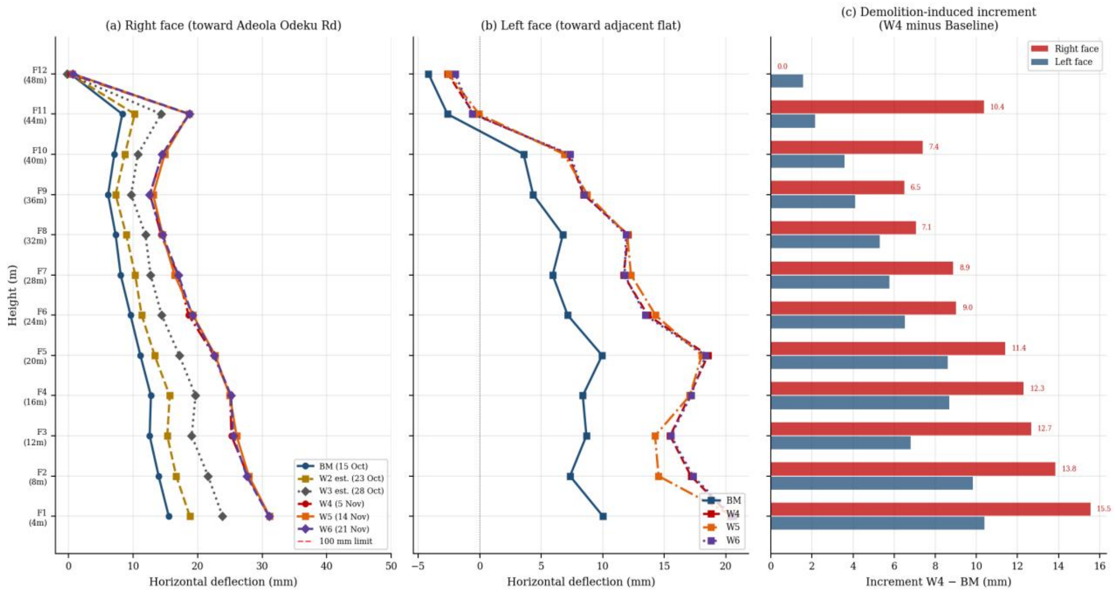

Figure 2. Total Station deflection profiles by floor level. (a) Right-face profiles all campaigns; (b) Left-face profiles; (c) Incremental deflection W4 minus baseline

(d) Multi-campaign bar chart; (e) Height–deflection polynomial regression (F1–F11); (f) Deflection growth rate BM→W4**.**

The Shapiro–Wilk test conducted on the baseline right-face deflections did not reject the null hypothesis of normality ($W = 0.91$, $p = 0.113 > 0.05$), suggesting that the data align with a normal distribution and justifying the subsequent use of parametric hypothesis tests.

4.2 Deflection Change During Active Demolition

Table 3 presents the cumulative Week 4 (W4) right-face displacements and their comparison to the BM2 baseline. The paired t-test yielded t-value of −8.03 ($df = 11$, $p = 6.3\times10^{-6}$). This highly statistically significant and correlates to deconstruction-induced structural displacement. The Wilcoxon signed-rank test with values of $W = 0$, and $p = 0.00098$ corroborated this finding. This is because under non-parameteric assumptions, a value of $W = 0$ statistically indicates that all 12 right-face floor displacements increased in the same direction between the two epochs. The mean rightward displacement increment was 9.58 mm, representing a 102.0% increase relative to the BM2 baseline mean of 9.39 mm, with a maximum increment of 15.55 mm recorded at Floor 2.

The second-order polynomial model fitted to the W4 epoch (Floors 1–11) is:

$$\delta\_W4(right) = 1.34\times10^{-2} \cdot H^2 - 1.054 \cdot H + 36.09 \qquad (3)$$

$$(R^2 = 0.909,\ n = 11,\ p < 0.001)$$

Comparison of the W4 and BM2 polynomial models reveals an increase in both the quadratic coefficient (from 5.55×10^{-3} to 1.34×10^{-2}) and the absolute magnitude of the linear coefficient (from 0.486 to 1.054), indicating a steeper and more strongly height-dependent displacement profile at W4. This evolution of the displacement profile is consistent with deconstruction-induced load redistribution altering the effective lateral stiffness distribution across the height of the structure, with the lower floors continuing to accumulate disproportionately larger displacements relative to the upper floors.

Table 3: Week 4 cumulative right-face deflections compared to baseline

Floor	Ht (m)	BM (mm)	W4 (mm)	Increment (mm)	Rate (mm/day)	% Change
1	4	15.53	31.08	+15.55	0.74	+100.1
2	8	13.96	27.81	+13.85	0.66	+99.2
3	12	12.57	25.24	+12.67	0.60	+100.8
4	16	12.76	25.06	+12.30	0.59	+96.4
5	20	11.13	22.54	+11.41	0.54	+102.5
6	24	9.60	18.61	+9.01	0.43	+93.9
7	28	8.08	16.95	+8.87	0.42	+109.8
8	32	7.29	14.34	+7.05	0.34	+96.7
9	36	6.13	12.62	+6.49	0.31	+105.9
10	40	7.09	14.49	+7.40	0.35	+104.4
11	44	8.32	18.68	+10.36	0.49	+124.5
12	48	0.27	0.27	0.00	0.00	0.0
Mean	—	9.39	18.97	+9.58	0.46	+102.0

4.3 Temporal Evolution and Growth Rate Analysis

Figure 3 presents the temporal evolution of right-face maximum and mean displacements across all measurement campaigns. Three distinct phases are identifiable in the displacement trajectory. First is a low-rate pre-deconstruction phase (days 0–13), during which maximum displacements increased from 15.53 mm at BM2 to approximately 22.6 mm at the reconstructed W3 epoch. This is followed by an accelerated displacement phase coinciding with the commencement of active deconstruction (days 13–21), during which displacements rose rapidly to 31.08 mm by W4. Lastly is a stabilization phase (days 21–37), during which week-on-week changes were less than 1 mm. During the stabilization phase, linear regression of the maximum displacement time series yielded a slope of 0.016 mm/day with $R^2 = 0.22$. The combination of a near-zero rate and low coefficient of determination (indicating that displacements varied with no systematic trend around a near-constant value), is consistent with near-complete structural stabilization at the prevailing deconstruction stage.

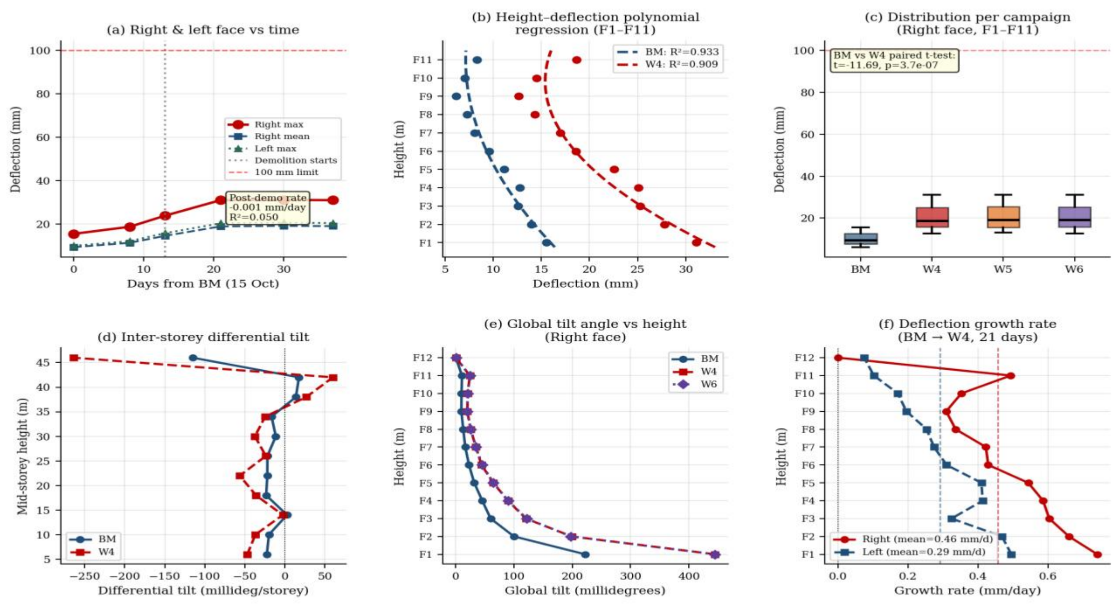

Figure 3. Temporal evolution of structural deflections. (a) Right-face maximum and mean vs time; (b) Left-face maximum vs time; (c) Campaign distribution (box plots); (d) Differential inter-storey tilt; (e) Global tilt vs height; (f) Cumulative displacement integral.

The mean displacement growth rate between BM2 and W4 was 0.46 mm/day on the right face and 0.29 mm/day on the left face. Floor 2 registered the highest right-face growth rate at 0.74 mm/day and also the highest left-face growth rate at approximately 0.50 mm/day, confirming that the lower floors experienced the most rapid displacement accumulation on both faces. Cohen's d effect sizes computed between the BM2 baseline and W6 were ≥ 0.8 (large effect threshold, per Cohen, 1988) for all floors on the right face. This confirms that the deconstruction-induced displacements are not only statistically significant but also of practical engineering magnitude.

4.4 Angular Deviation and Tilt Analysis

The global tilt angles on the right face was calculated using equation (4)

$$\theta = tan^{-1}\frac{\delta}{H} \qquad (4)$$

where δ is the measured horizontal displacement in mm and H is the floor height in mm,

From the analysis, the tilt angles went from a maximum of 0.222° at Floor 2 under baseline conditions to 0.445° at Week 4. This is almost double the amount of structural lean at the lowest monitored floor. The differential tilt profile shows that the angle between Floors 1 and 2 changes the most, and that there is a second change from the main trend between Floors 9 and 11. This means that there are localized areas of differential displacement in both the lower and upper-middle parts of the structure (Figure 4).

At baseline, the right-face angular deviations were between 2.0 and 9.8 arcseconds, and at Week 4, they were between 4.1 and 19.8 arcseconds. The horizontal observation distances stayed the same across all campaigns, between 39.0 and 47.6 m. The Pearson correlation coefficient between floor height and baseline right-face angular deviation was r = −0.930 (p < 0.001), corroborating the prevailing monotonic decline in angular deviation as height increases.

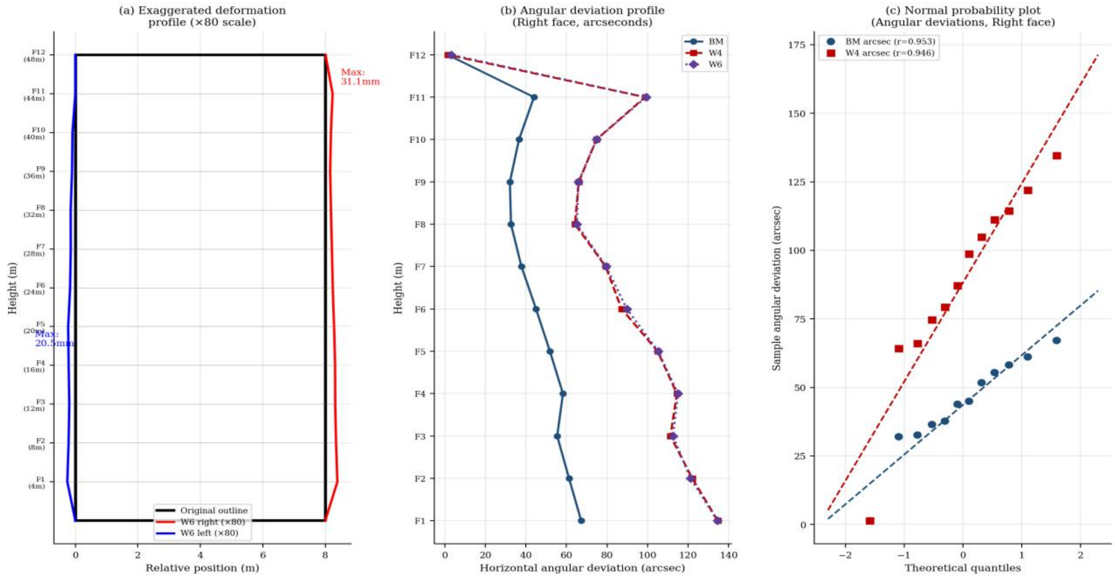

Figure 4. Deformation field and angular deviation analysis. (a) Exaggerated deformation profile (×80 scale); (b) Angular deviation in arc-seconds vs height; (c) Deflection vectors at selected floors.

4.5 Spatial Displacement Field

The inter-campaign Pearson correlation matrix reveals strong positive correlations between BM2 and W4 ($r = 0.99$, $p < 0.0001$), and between W4 and both W5 and W6 ($r > 0.99$). This indicates that the spatial distribution of displacements remained consistent across all epochs while only the magnitudes changed (Figure 5). This persistent spatial consistency suggests that the structure continued to accumulate displacement in a stable deformation pattern throughout the monitoring period, rather than developing any progressive change in the distribution of lateral displacement that would indicate the onset of a new or evolving failure mechanism.

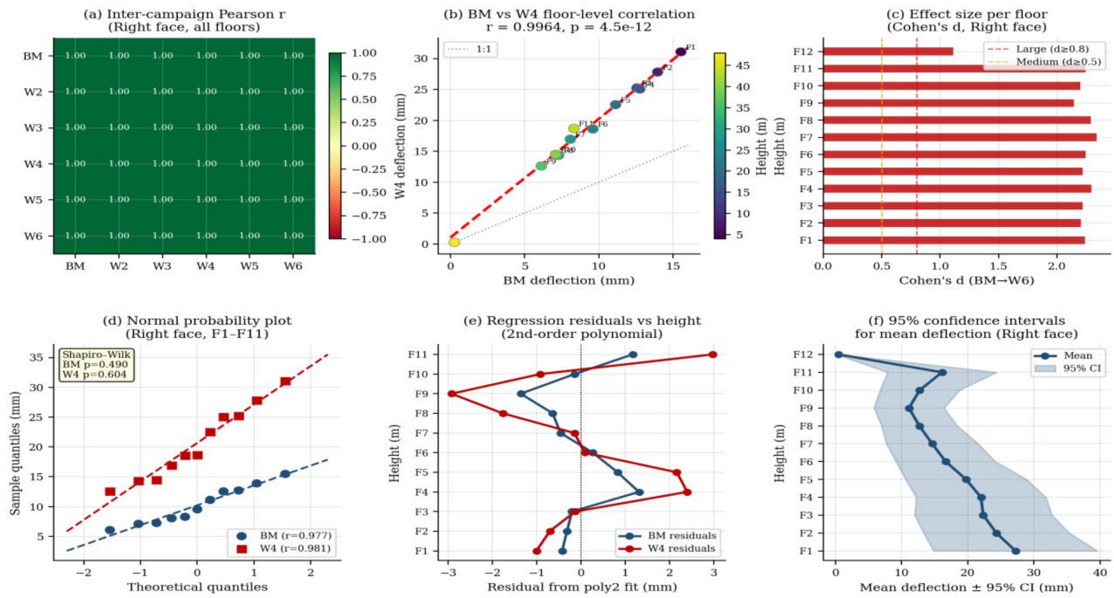

Figure 5. Statistical characterization of Total Station measurements. (a) Inter-campaign correlation matrix; (b) BM vs W4 scatter; (c) Regression residuals vs height; (d) Normal probability plots with Shapiro–Wilk results; (e) Cohen's d effect sizes per floor; (f) 95% confidence intervals for mean deflection.

4.6 Safety Threshold Assessment

The maximum displacement recorded during all campaigns was 31.08 mm at Floor 2 on the right face during Week 4. This is 31.1% of the 100 mm safety threshold that was set. There were two possible projection scenarios. With a stable post-W4 growth rate of 0.016 mm/day, the safety threshold would not be reached for about 4,300 days after Week 6, which is much longer than the expected time for deconstruction. If we assume that the active-phase W4 growth rate of 0.46 mm/day stays the same, which is more conservative, the threshold would be reached about 148 days after the Week 4 measurement. Both scenarios show that the current method of deconstruction keeps the levels of displacement safely within the safety envelope. However, these projections depend on the current top-down, low-vibration deconstruction methods continuing. If active deconstruction were to move down to the sub-penthouse floor levels, it would change the structural loading conditions significantly and require a new look at the projected displacement trajectory.

4.7 Nature of Pre-Existing Structural Deformation

The parabolic displacement profile seen at baseline ($R^2 = 0.933$), which has the most displacement at the lowest monitored floor and a clear monotonic decrease with height, is in line with lateral deformation that is mostly concentrated in the lower part of the structure. In a classical top-loaded lateral response of an undamaged frame, the biggest displacements would happen on the upper floors. This pattern is different. Instead, the observed distribution is more in line with differential deformation at or near the foundation level, or with localized loss of lateral stiffness in the lower column elements. This would create a displacement field that is strongest at the base and gets weaker as you go up. In a healthy RC frame with uniform lateral loading, each floor would add about the same amount to the total lateral displacement. However, the concentration at lower floors seen here is very different from what was expected.

The secondary displacement increase at Floors 10–11, which goes against the overall trend of decrease, suggests that there is a localized area of the structure where the stiffness changes differently in the upper-middle section. This could be due to pre-existing cracks, loss of localized sections, or uneven vertical load distribution at those levels.

The inter-campaign Pearson correlation matrix with $r > 0.99$ between all post-BM2 campaigns shows that the spatial distribution of displacements stayed the same during the monitoring period, and only the magnitudes changed. This consistent spatial pattern shows that the structure kept getting more displacement in the same direction across all campaigns. It didn't show any signs of a new or evolving failure mechanism by redistributing lateral displacement in a way that would suggest it was changing.

4.8 Demolition-Induced Deflection Increment

The increase in right-face displacements from baseline to W4 of about 102% is much bigger than what would be expected from the direct dynamic effects of the jack-hammer operations alone. The theoretical dynamic analysis could be an indication that the primary jack-hammer excitation frequency of roughly 9.5 Hz yields Dynamic Magnification Factors ranging from 0.019 to 0.057 at the monitored floor levels, thereby confirming that the direct vibrational impact on structural displacement is minimal. The observed quasi-static increment is due to the gradual redistribution of structural loads after the penthouse mass is removed. This changes the way the underlying structural frame is loaded.

The stabilization of displacements between W5 and W6, with week-on-week changes of less than 1 mm, indicates that the structure has reached a new quasi-static equilibrium under the reduced loading state after the partial removal of the penthouse. This behavior is physically anticipated because, when a structure with accumulated inelastic deformation is partially unloaded, the recoverable elastic component is released while the irrecoverable plastic component is preserved. This leads to a new stable displaced configuration.

4.9 Safety Assessment and Monitoring Implications

The highest recorded displacement of 31.08 mm at Floor 2 (right face, W4) is 31.1% of the 100 mm safety threshold that was set. All displacements across all campaigns stayed within the safety envelope. The fact that all of the displacement vectors keep pointing toward the right and forward faces of the structure is important for safety because the critical displacement path is pointing toward the nearest building. This means that it is especially important to keep an eye on that face as deconstruction moves down to the sub-penthouse floor levels. The consistent direction of the observed displacement field strongly supports the idea of adding lateral restraint to that side of the building before the lower floors are taken down.

Also, It is important to pay close attention to the fact that there is no measurable displacement increment at Floor 22 between BM2 and W4. This floor is right below the area where the penthouse is being taken down. The fact that there is no positive increment, which is different from what happens on all the other floors, suggests that the local structural constraint conditions at Floor 22 have changed because the penthouse mass above has been removed. This could have happened by relieving the compressive pre-stress in the columns at that level. As deconstruction work gets closer to Floor 22, this behavior should be watched closely.

5. CONCLUSION

This study shows the capability of a Total Station geodetic monitoring observation framework for reliable and independently verifiable evaluation of structural safety during controlled deconstruction of high-rise reinforced concrete buildings in complicated urban settings. The results show that quasi-static displacement accumulation, which cannot be measured accurately with vibration-based sensing alone, can be described with enough accuracy to find statistically significant structural responses, measure directional displacement trends, and set safety margins against set thresholds. The persistent spatial consistency of the displacement field across all campaigns further illustrates that geodetic monitoring can differentiate stable progressive deformation from the initiation of lateral instability. This distinction is essential for operational safety decision-making in densely constructed environments.

The methodology and analytical framework developed herein is also applicable for structural health monitoring practices across Nigeria, where regulated deconstruction of aging and structurally evaluated buildings presents a growing urban engineering challenge, yet is inadequately substantiated by documented field evidence. The combined use of polynomial displacement modeling, tilt angle measurement, and effect size analysis with traditional hypothesis testing creates a model that can be used in future monitoring campaigns. The geodetic dataset produced is a validated baseline that can be used to compare the results of other independent monitoring techniques.

REFERENCES

Carden, E. P., & Fanning, P. (2004). Vibration based condition monitoring: A review. *Structural Health Monitoring, 3*(4), 355–377. https://doi.org/10.1177/1475921704047500

Cohen, J. (1988). *Statistical power analysis for the behavioral sciences* (2nd ed.). Hillsdale, NJ: Lawrence Erlbaum Associates.

Doebling, S. W., Farrar, C. R., & Prime, M. B. (1998). A summary review of vibration-based damage identification methods. *The Shock and Vibration Digest, 30*(2), 91–105.

Fan, H., Peng, H., Li, W., & Huang, Q. (2020). Measurement of quasi-static and dynamic displacements of footbridges using the composite instrument of a SmartStation and an accelerometer. *Remote Sensing, 12*(16), 2635. https://doi.org/10.3390/rs12162635

Farrar, C. R., & Worden, K. (2007). An introduction to structural health monitoring. *Philosophical Transactions of the Royal Society A: Mathematical, Physical and Engineering Sciences,* 365(1851), 303–315. https://doi.org/10.1098/rsta.2006.1928

International Organization for Standardization. (2017). *Accuracy in building — Part 1: Methods for measurement and evaluation* (ISO 7976-1:2017). Geneva, Switzerland: Author.

Lienhart, W. (2017). Geotechnical monitoring using total stations and laser scanners: Critical aspects and solutions. *Journal of Civil Structural Health Monitoring, 7*(3), 315–324. https://doi.org/10.1007/s13349-017-0228-5

Scaioni, M., Marsella, M., Crosetto, M., Tornatore, V., & Wang, J. (2018). Geodetic and remote-sensing sensors for dam deformation monitoring. *Sensors, 18*(11), 3682. https://doi.org/10.3390/s18113682

Yuzbasi, J. (2025). Fundamentals of Controlled Demolition in Structures: Real-Life Applications, Discrete Element Methods, Monitoring, and Artificial Intelligence-Based Research Directions. *Buildings, 15*(19), 3501. https://doi.org/10.3390/buildings15193501